Title Page

Polymorphic Human Sulfotransferase 2A1 Mediates the Formation of 25-Hydroxyvitamin D_3-3-*O*-sulfate, A Major Circulating Vitamin D Metabolite in Humans

Timothy Wong, Zhican Wang, Brian D. Chapron, Mizuki Suzuki, Katrina G. Claw, Chunying Gao, Robert S. Foti, Bhagwat Prasad, Alenka Chapron, Justina Calamia, Amarjit Chaudhry, Erin G. Schuetz, Ronald L. Horst, Qingcheng Mao, Ian H. de Boer, Timothy A. Thornton, and Kenneth E. Thummel

Departments of Pharmaceutics (T.W., Z.W., M.S., K.C., C.G, B.P., Ale.C., B.C., Q.M, J.C. and K.T.), Medicine and Kidney Research Institute (I.B.), and Biostatistics (T.T.), University of Washington, Seattle, WA, United States

Department of Pharmacokinetics and Drug Metabolism, Amgen Inc., South San Francisco (Z.W.), CA, and Cambridge (R.F.), MA, United States

St Jude Children's Research Hospital (A.C. and E.S.), Memphis, TN, United States

Heartland Assays (R.H.), LLC, Ames, Iowa, United States

Running Title Page

Running title: Sulfonation of 25-hydroxyvitamin D_3

Corresponding author:

Kenneth E. Thummel, Ph.D., Department of Pharmaceutics, Box 357610, University of Washington, Seattle, WA 98195-7610. Phone: 206-543-0819, FAX: 206-543-3204, email: thummel@u.washington.edu

Number of text pages: 42

Number of tables: 2

Number of figures: 8

Number of supplemental tables: 2

Number of supplemental figures: 4

Number of references: 64

Number of words in the Abstract: 243

Number of words in the Introduction: 540

Number of words in the Discussion: 1492

Abbreviations

BSA: bovine serum albumin; DAPTAD: 4-(4'-dimethylaminophenyl)-1,2,4-triazoline-3,5-dione; DBP: vitamin D binding protein; DMSO: dimethyl sulfoxide; DHEA: dehydroepiandrosterone; ESI: electrospray ionization; IS: internal standard; LC-MS: liquid chromatography-mass spectrometry; 25OHD3: 25-hydroxyvitamin D_3; PAPS: 3-phosphoadenosine-5-phosphosulfate; PTAD: 4-phenyl-1,2,4-triazoline-3,5-dione; SPE: solid phase extraction; PXR: pregnane X receptor; SULT: sulfotransferase; vitamin D_3: cholecalciferol; vitamin D2: ergocalciferol

Abstract

Metabolism of 25-hydroxyvitamin D_3 ($25OHD_3$) plays a central role in regulating the biological effects of vitamin D in the body. Although cytochrome P450-dependent hydroxylation of $25OHD_3$ has been extensively investigated, limited information is available on the conjugation of $25OHD_3$. In the present study, we report that $25OHD_3$ is selectively conjugated to $25OHD_3$-3-*O*-sulfate by human sulfotransferase 2A1 (SULT2A1) and that the liver is a primary site of metabolite formation. At a low (50 nM) concentration of $25OHD_3$, $25OHD_3$-3-*O*-sulfate was the most abundant metabolite, with an intrinsic clearance approximately 8-fold higher than the next most efficient metabolic route. In addition, $25OHD_3$ sulfonation was not inducible by the potent hPXR agonist, rifampicin. The $25OHD_3$ sulfonation rates in a bank of 258 different human liver cytosols were highly variable, but correlated with the rates of dehydroepiandrosterone sulfonation. Further analysis revealed a significant association between a common SNV within intron-1 of *SULT2A1* (rs296361; MAF = 15% in Whites) and liver cytosolic SULT2A1 content as well as $25OHD_3$-3-*O*-sulfate formation rate, suggesting that variation in the *SULT2A1* gene contributes importantly to inter-individual differences in vitamin D homeostasis. Finally, $25OHD_3$-3-*O*-sulfate exhibited high affinity for the vitamin D binding protein and was detectable in human plasma and bile, but not in urine samples. Thus, circulating concentrations of $25OHD_3$-3-*O*-sulfate appear to be protected from rapid renal elimination, raising the possibility that the sulfate metabolite may serve as a reservoir of $25OHD_3$ *in vivo*, and contribute indirectly to the biological effects of vitamin D.

Introduction

Vitamin D deficiency has been associated with a wide range of adverse health outcomes, such as rickets, osteoporosis, diabetes, multiple sclerosis, and colon cancer (Holick, 2007), although evidence for non-skeletal effects is more limited than that for skeletal disease (Theodoratou et al., 2014). Vitamin D is found in nature in the forms of cholecalciferol (vitamin D_3) and ergocalciferol (vitamin D_2), with predominately vitamin D_3 in untreated humans. 25-hydroxyvitamin D_3 ($25OHD_3$), a major circulating metabolite of vitamin D_3, is used as a clinical biomarker for assessment of vitamin D status; concentrations < 20 ng/mL (50 nM) are considered insufficient for bone health by the Institute of Medicine (Hossein-nezhad and Holick, 2013) and deficient by others (Holick et al., 2011). Multiple factors affect vitamin D sufficiency, including the synthesis of vitamin D_3 in the skin, the absorption of vitamin D_3 and D_2 from food in the intestine, vitamin D 25-hydroxylation activity in the liver and a combination of 25OHD oxidation and conjugation reactions catalyzed principally in the kidney, liver and small intestine (DeLuca, 1988; Jones et al., 2014).

Variation in the diet and exposure to sunlight contribute importantly to intra- and inter-individual differences in serum $25OHD_3$ concentration, but much of the observed variance remains unexplained (Fuleihan Gel et al., 2015). Results from genome-wide and candidate gene association studies have implicated *CYP2R1*, *CYP24*, *GC* (plasma vitamin D binding protein) and *DHCR7* gene variation in serum $25OHD_3$ variability, but the extent of their contribution appears low (Ahn et al., 2010; Bu et al., 2010; Berry and Hypponen, 2011) despite $25OHD_3$ heritability estimates of 20-85% (Hunter et al., 2001; Arguelles et al., 2009; Shea et al., 2009).

$25OHD_3$-3-*O*-sulfate is reported to be a major circulating metabolite of $25OHD_3$ in humans, with an average circulating concentration comparable to that of $25OHD_3$ (Axelson,

1985; Shimada et al., 1995; Higashi et al., 2014), and thus, the sulfonation metabolic pathway might contribute importantly to vitamin D homeostasis. Surprisingly, little is known about how and where 25OHD$_3$-3-*O*-sulfate is formed. This information is crucial if contribution from the sulfonation pathway to vitamin D homeostasis is to be fully evaluated. In this study, we examined the sulfonation of 25OHD$_3$ in humans using recombinant SULT enzymes, liver cytosols, primary hepatocytes, renal tubular epithelial cells and immortalized intestinal epithelial cells to identify which of the human SULTs is responsible for the sulfonation reaction and in what tissues the reaction occurs, as well as potential genetic and environmental sources of interindividual variability in hepatic sulfonation activity.

The formation of 25OHD$_3$-3-*O*-sulfate from 25OHD$_3$ could be considered a catabolic process, but some investigators have hypothesized that it also represents an alternative 25OHD$_3$ storage form in the body (Higashi et al., 2010). This is quite plausible because other endogenous steroid sulfate conjugates, such as estradiol-sulfate and dehydroepiandrosterone (DHEA)-sulfate, circulate at relatively high levels, are de-conjugated in target tissues and contribute to certain physiological functions (Axelson, 1987; Banerjee et al., 2013; Sanchez-Guijo et al., 2015). Similarly, 25OHD$_3$-3-*O*-sulfate might be retained in circulation and distributed to different tissues of the body where it could be hydrolyzed to 25OHD$_3$, replenishing the 25OHD$_3$ pool, as needed. With this in mind, we also tested the binding affinity of 25OHD$_3$-3-*O*-sulfate for vitamin D binding protein (DBP) and its presence in human urine and bile.

Materials and Methods

Materials

DMD Fast Forward. Published on January 17, 2018 as DOI: 10.1124/dmd.117.078428
This article has not been copyedited and formatted. The final version may differ from this version.

Chemicals. DHEA, 3-phosphoadenosine-5-phosphosulfate (PAPS), 4-phenyl-1,2,4-triazoline-3,5-dione (PTAD), and rifampicin were purchased from Sigma-Aldrich (St. Louis, MO, USA). The precursors of 4-(4'-dimethylaminophenyl)-1,2,4-triazoline-3,5-dione (DAPTAD) were obtained as follows: 4-(4'-dimethylaminophenyl)-1,2,4-triazolidine-3,5-dione (Santa Cruz Biotechnology, Dallas, TX) and iodobenzene diacetate (Sigma, St. Louis). $25OHD_3$ was obtained from Calbiochem (La Jolla, CA) and its deuterated form, d_6-$25OHD_3$ (containing six deuterium atoms at C-26 and C-27) was purchased from Medical Isotope Inc. (Pelham, NH). Chemically synthesized $25OHD_3$-3-*O*-sulfate and its deuterated form, d_6-$25OHD_3$-3-*O*-sulfate, were purchased from Toronto Research Chemicals (Ontario, Canada). $25OHD_3$-25-*O*-glucuronide and its deuterated form were generated by enzymatic reactions, isolated and purified as described (Gao et al., 2017). All other buffers and chemicals were of the highest grade commercially available.

Sequencing grade trypsin, iodoacetamide, dithiothreitol and bovine serum albumin (BSA) were purchased from Pierce Biotechnology (Rockford, IL). Two synthetic surrogate peptides (Supplementary Table 1) for both SULT2A1 and BSA were identified using the published protocol (Prasad and Unadkat, 2014a; Prasad and Unadkat, 2014b) and procured from Thermo Fisher Scientific (Rockford, IL). Chloroform, HPLC-grade acetonitrile, methanol and formic acid were purchased from Fischer Scientific (Fair Lawn, NJ). Ammonium bicarbonate (98% purity) and sodium deoxycholate (98% purity) were obtained from Thermo Fisher Scientific (Rockford, IL) and MP Biomedicals (Santa Ana, CA), respectively.

Cell culture medium, insulin-transferrin-selenium-A, penicillin-streptomycin and amphotericin B were purchased from Invitrogen (Carlsbad, CA). Fetal bovine serum (FBS) was obtained from Atlanta Biologicals (Lawrenceville, GA). Sodium pyruvate was purchased from

Cellgro (Herndon, VA). Hydrocortisone and cell dissociation solution was purchased from Sigma. Mouse collagen IV was obtained from Corning (Corning, NY).

Human recombinant enzymes and cells. For the SULT isoform activity screening experiments, human recombinantly expressed SULT isoforms SULT1A1, SULT1B1, SULT1E1, SULT2A1, and SULT2B1 were purchased from Genway Biotech (San Diego, CA). For kinetic experiments, purified recombinant SULT2A1 was purchased from R&D Systems (Minneapolis, MN). This same product was used as an authentic standard to determined the SULT2A1 specific content of pooled human liver cytosol. Cryopreserved primary human hepatocytes from two different human liver donors were obtained from either Triangle Research Labs (lot no. GC4008; Caucasian male; age 69; no alcohol, tobacco, or drug use) (Durham, NC), or Invitrogen (lot no. Hu4237; Caucasian female; age 57; no alcohol, tobacco, or drug use) (Carlsbad, CA), and cultured as previously published (Wang et al., 2013a). The human intestinal epithelial LS180 cell line was obtained from ATCC (Manassas, VA). Human renal cortical tissue was obtained during the surgical resection of a renal cell carcinoma. Renal tubular epithelial cells were isolated from a non-cancerous section of tissue from three donors using established methods (Weber et al., 2016). The surgery was performed at the University of Washington Medical Center and the human subjects protocol was approved by the University of Washington Human Subjects Review Board.

Tissue samples. A total of 258 human livers from the University of Washington School of Pharmacy Human Tissue Bank, a resource established by a Program Project grant on Drug Interactions from the National Institutes of Health (P01-GM32165), and the St Jude Liver Resource human liver tissues [obtained through the Liver Tissue Cell Distribution System, Minneapolis, Minnesota and Pittsburgh, Pennsylvania and funded by NIH Contract #

HHSN276201200017C (Shirasaka et al., 2015)], were used for this investigation. The collection and use of these tissues for research purposes was approved by the Human Subjects Institutional Review Boards at the University of Washington and St. Jude Children's Research Hospital. In both cases, all links between archived tissues and the original donors were destroyed to preserve anonymity and facilitate research. The liver bank donors were: 44% female, 56% male; ages <1 – 81 years, mean = 43 years; 93% White European ancestry, 4% Black, 1% Hispanic and 2% unknown.

Outdated human plasma was from the Puget Sound Blood Center (Seattle, WA); anonymous, pooled human bile was kindly provided by Dr. Evan D. Kharasch at the Washington University in St. Louis (St. Louis, MO); and anonymous pooled human urine was collected at the University of Washington. These outdated human samples were analyzed under an institution exempt approval from the University of Washington Human Subjects Review Board.

DNA and RNA for DNA-Seq and RNA-Seq analysis were isolated from liver tissue, as described below. Cytosolic fractions were isolated, as previously described (Shirasaka et al., 2015). Sulfonation activity measurements are described below. Total protein concentration in each cytosol preparation was measured by bicinchoninic acid assay (Thermo Scientific, IL).

Formation of 25OHD$_3$-3-*O*-sulfate by pooled human liver cytosol and recombinant SULT isozymes

The following procedures were conducted under low light conditions to avoid potential degradation of vitamin D metabolites. Initial experiments with liver cytosols or SULTs (SULT1A1, SULT1B1, SULT1E1, SULT2A1, and SULT2B1) were carried out in 50 mM Tris-HCl (pH 7.5) solution containing 1 mg/mL pooled liver cytosols or 0.025 mg/mL recombinant SULT, 5 μM 25OHD$_3$ and 0.1 mM PAPS, with a 0.5 mL final volume in glass tubes. Briefly,

pooled liver cytosols (n = 10, randomly selected from 266) or SULT enzyme were mixed with $25OHD_3$ and pre-warmed at 37 °C for 5 min. The reaction was initiated by adding PAPS and maintained at 37 °C for various times as indicated, and terminated with an equal volume of ice-cold acetonitrile. Incubations without PAPS served as negative controls.

Kinetic studies were conducted in 50 mM Tris-HCl (pH 7.5) solution containing pooled liver cytosol (1 mg/mL; 0.2 mg in 0.2 mL final volume) or recombinant SULT2A1 (0.025 mg/mL purified SULT2A1 (2.5 µg SULT2A1 in 0.1 mL final volume) under conditions (worked out in pilot studies) that provided linear product formation with respect to protein concentration and time. The range of substrate concentration was 0.25 – 40 µM for $25OHD_3$ and each incubation was conducted at 37 °C for 30 min. Reactions were initiated with addition of 0.1 mM PAPS and terminated with the addition of two volumes of ice-cold acetonitrile (0.4 mL for cytosol and 0.2 mL for SULT2A1 incubations) containing internal standard d_6-$25OHD_3$-3-*O*-sulfate (100 nM) and the mixtures were transferred to Eppendorf tubes and centrifuged for 5 min (12,000*g*). The supernatants were collected, concentrated under a nitrogen stream, and reconstituted in 20% acetonitrile in mobile phase for LC-MS analysis (see below). Incubations without PAPS served as negative controls.

The rates of product formation were normalized for SULT2A1 or cytosolic protein concentration. We also determined the specific SULT2A1 content of the pooled human liver cytosol preparation (see below) and normalized the cytosolic rates for the SULT2A1 specific content. A simple Michaelis-Menten kinetics model was fit to each $25OHD_3$ data set using nonlinear regression data analysis (GraphPad Prism v.5, La Jolla, CA). Each experimental reaction condition was conducted in duplicate (technical replicate) and repeated three times

independently (different days) to generate mean and variance for kinetic parameters: K_m and V_{max}.

Formation of 25OHD$_3$-3-sulfate and DHEA-sulfate by a panel of human liver cytosols

To characterize and compare inter-individual differences in hepatic 25OHD$_3$ and DHEA sulfonation activity, we incubated 266 individual human liver cytosol preparations (0.25 mg/mL) in 50 mM Tris-HCl (pH 7.5), 5 µM 25OHD$_3$ or DHEA (established probe substrate for SULT2A1), and 0.1 mM PAPS, with a 0.1 mL final volume (0.025 mg protein) in glass tubes. After pre-warming the mixture at 37 °C for 5 min, the reaction was initiated by adding PAPS and maintained at 37 °C for 30 min and terminated with addition of an equal volume of ice-cold acetonitrile. Once again, incubations without PAPS served as negative controls. Rates of product formation were normalized for cytosolic protein concentration.

Formation of 25OHD$_3$-3-*O*-sulfate and other 25OHD$_3$ metabolites in human cell cultures

Cryopreserved human hepatocytes from two donors were thawed and cultured, as previously published (Wang et al., 2013a). After plating and culturing of viable cells in Collagen I coated 96-well plates for 24 hours, the cells were treated with 10 µM rifampicin or vehicle, 0.1% dimethyl sulfoxide (DMSO), in a 100 µL solution per well. After 48 hours, the treated cells were washed with saline solution twice and then incubated with 50 nM 25OHD$_3$ for various incubation times (t = 2, 4, 8 or 24 hours). At the end of the treatment period, culture medium was collected from 12 wells and pooled, if necessary.

For quantitation of 25OHD$_3$ oxidative metabolites, cell medium samples (0.5 mL) were subjected to liquid-liquid extraction with addition of 5 mL ethyl acetate, followed by PTAD derivatization and reconstitution in 40% acetonitrile containing 0.1% formic acid. Formation of both 4β,25(OH)$_2$D$_3$ and 4α,25(OH)$_2$D$_3$ was quantified after treatment of the cell culture medium

with β-glucuronidase (1500 IU/mL) prior to the liquid-liquid extraction step in order to account for significant secondary metabolism, as previously described (Wang et al., 2013a). For quantification of 25OHD$_3$-glucuronides, cell medium (0.25 mL) were quenched with 2 volumes of ice-cold acetonitrile, and the mixtures were centrifuged at 12,000*g* for 4 min in Eppendorf tubes (Wang et al., 2014). The supernatants were collected, concentrated under a nitrogen stream, and reconstituted in 50 µL mobile phase (20% acetonitrile in 5 mM ammonium acetate) for LC-MS analysis as described below.

For quantitation of 25OHD$_3$-3-*O*-sulfate, cell medium samples (0.3 mL) were buffered with an equal volume of 0.1 M sodium acetate (pH 4.0) and subjected to solid-phase extraction using a Waters Oasis WAX (30 mg, 1 cc) anion exchange cartridges, under conditions suggested by the manufacturer. Briefly, Oasis cartridges were pre-conditioned with methanol and 2% acetic acid before loading of diluted samples. After loading, cartridges were washed with 2% acetic acid and 100% methanol sequentially. 25OHD$_3$-3-*O*-sulfate was eluted by 3 mL of buffer containing a mixture of 5:95 (v/v) ammonium hydroxide (28%) to methanol. The eluates were dried, pooled if necessary, and reconstituted in 50 µL mobile phase solution (20% acetonitrile in 5 mM ammonium acetate) for LC-MS analysis as described below.

In order to assess the conversion of 25OHD$_3$ to 25OHD$_3$-3-*O*-sulfate at extrahepatic sites that are important in maintaining systemic vitamin D homeostasis, additional experiments were performed using human renal tubular epithelial cells from three different tissue donors and the LS180 colon carcinoma cell line. LS180 cells (passage 30) and human renal tubule epithelial cells (passage 4) were cultured on uncoated and collagen IV-coated 6-well plates respectively for 1 week. The cells were then washed with saline solution twice and incubated with 50 nM

$25OHD_3$. Culture medium was collected after 24 hours and concentrations of $25OHD_3$-3-*O*-sulfate were quantified using the same LC-MS method, as described for hepatocytes

Quantitation of $25OHD_3$-3-*O*-sulfate in recombinant SULT enzyme, human cytosol and cell incubates

Samples reconstituted in mobile phase (20% acetonitrile in 5 mM ammonium acetate, pH 4.6; 15 µL injected on column) were subjected to LC-UV/MS analysis using an Agilent MSD mass spectrometer coupled with an Agilent 1100 series HPLC system. Chromatographic separation was achieved on a Symmetry C18 (2.1 mm × 150 mm, 3.5 µm) column (Waters, Milford, WA) and a mobile phase consisting of 5 mM ammonium acetate (A, pH 4.6) and acetonitrile (B) at 45 ^oC. A linear gradient from 20% B (0 – 2 min) to 90% B (17 – 22 min) in 15 min at 0.25 mL/min flow rate was employed. UV detection was performed at 265 nm. The mass spectrometer was operated in the negative ionization mode. The interface was maintained at 350 ^oC with a nitrogen nebulization pressure of 25 psi, resulting in a flow of 10 L/min. $25OHD_3$-3-*O*-sulfate and d_6-$25OHD_3$-3-*O*-sulfate were detected by selective ion monitoring at *m/z* 479 and 485, respectively, following 110 V ion fragmentation. $25OHD_3$-3-*O*-sulfate eluted from the column at approximately 14.4 min. Calibration curves were constructed by plotting the peak area ratios of $25OHD_3$-3-*O*-sulfate and d_6-$25OHD_3$-3-*O*-sulfate versus the corresponding $25OHD_3$-3-*O*-sulfate concentrations and fitting a linear regression equation to the data. Formation of $25OHD_3$-3-*O*-sulfate was then quantified by fitting the peak area ratios (metabolites/internal standard) from incubations to the calibration curve.

Quantitation of $25OHD_3$ monohydroxy and glucuronide metabolites in human hepatocyte incubations

Quantification of 25OHD$_3$ monohydroxy metabolites and primary glucuronides was performed using previously published LC-MS/MS (Wang et al., 2013a) and LC-MS (Wang et al., 2014) methods, respectively. Briefly, LC-MS/MS was performed using an Agilent 1290 series UPLC and an Agilent 6410 triple quadrupole tandem mass spectrometer equipped with an electrospray ionization source (Pala Alto, CA). Separation was achieved on a Hypersil Gold (2.1 × 100 mm, 1.9 µm) column, and the Multiple Reaction Monitoring (MRM) of the transitions *m/z* 574 → 314, 574 → 298, 558 → 298, 564 → 298 and 580 → 314 were employed to detect 1α (4α or 4β),25(OH)$_2$D$_3$, 24,25(OH)$_2$D$_3$, 25OHD$_3$, d$_6$-25OHD$_3$ and d$_6$-1α,25(OH)$_2$D$_3$, respectively (Wang et al., 2013a). Calibration curves were constructed by plotting the peak area ratio for each vitamin D$_3$ metabolite and its internal standard, versus the corresponding concentration, and fitting a linear regression equation to the data. LC/MS analysis was performed using an Agilent MSD mass spectrometer coupled with an Agilent 1100 series LC system (Wang et al., 2014). Chromatographic separation was achieved on a Symmetry C18 (2.1 mm × 150 mm, 3.5 µm) column (Waters, Milford, WA). Separations were achieved after a linear gradient from 30% B (2 min) to 45% B (25 min), hold at 45% B for 1 min and increased to 60% B (35 min), increased to 90% in 1 min and hold for 3 min (39 min), and then equilibrated back to 30% B in 1 min. 25OHD$_3$ glucuronides and d$_6$-25OHD$_3$-25-glucuronide as the internal standard were detected by selective ion monitoring at *m/z* 575 and 581, respectively, following 110 V ion fragmentation. Calibration curves were constructed by plotting the peak area ratio of glucuronide metabolites and internal standard versus the corresponding standard 25OHD$_3$-25-glucuronide concentration and fitting a linear regression equation to the data.

Quantitation of 25OHD$_3$-3-*O*-sulfate in human plasma, bile and urine

Human plasma (0.1 mL) and urine (0.5 mL) were first subjected to protein precipitation using two volumes of acetonitrile followed by dilution with two volumes of 0.1 M sodium acetate (pH 4.0). For human bile (1 mL), the pooled (from different adult donors) sample was first diluted with 0.5 mL water, subjected to liquid-liquid extraction using an equal volume of hexane, twice. The aqueous solution was separated, pooled if necessary, and buffered with an equal volume of 0.1 M sodium acetate (pH 4.0) and subjected to solid-phase anion exchange extraction of 25OHD$_3$-3-*O*-sulfate, using the Waters Oasis WAX (60 mg, 3 cc) anion exchange cartridges, as described above (cell culture experiments). After solid phase extraction, the eluate was transferred to a new glass tube, dried and reconstituted in 50 µL of 20% acetonitrile in 5 mM ammonium acetate. Reconstituted samples were analyzed for 25OHD$_3$-3-*O*-sulfate concentration, as described above for quantitation 25OHD$_3$-3-*O*-sulfate produced during *in vitro* incubations. The limit of in plasma and urine was estimated at 1.0 ng/mL with intra- and inter-day errors of $\leq$ 15%.

For better detection of 25OHD$_3$-3-*O*-sulfate in bile samples, a derivatization step was included as part of the sample treatment following a previously reported method (Gao et al., 2017). Briefly, pooled human bile (100 µL) was precipitated with 200 µL acetonitrile and buffered with 1 mL of 0.1 M sodium acetate (pH 3.2) and subjected to SPE using the Waters Oasis WAX (60 mg, 3 cc) anion exchange cartridges. The eluates from SPE were then dried and reconstituted in 10 µL methanol and derivatized with 200 µL of 4.5 mM DAPTAD solution for 1 hr at room temperature in the dark (Ogawa et al., 2013). The reaction mixture was then evaporated under N_2 flow and reconstituted in 100 µL mobile phase. A centrifugation step was included to remove an insoluble substance before LC-MS/MS analysis. DAPTAD-25OHD$_3$-3-*O*-sulfate was analyzed using an AB Sciex QTRAP 6500 LC-MS/MS system. Chromatographic

separation was achieved on a Hypersil Gold (2.1 × 100 mm, 1.9 μm) column (Thermo Scientific) and a mobile phase consisting of 5 mM ammonium acetate (A, pH 4.6) and acetonitrile (B) at 45 ˚C. Linear gradients were applied with B% increased from 25 to 60% B (1 – 13 min) and from 60 to 90% (13-16 min) at 0.25 mL/min flow rate. The autosampler was maintained at 4 ˚C and the injection volume was 15 μL. The electrospray ionization (ESI) source of the mass spectrometer was operated in the positive ion mode. Detection was by multiple reaction monitoring (MRM) of the transitions at m/z 699.5→323 for DAPTAD-25OHD$_3$-3-*O*-sulfate and m/z 705.5 → 323 for the internal standard DAPTAD-d$_6$-25OHD$_3$-3-*O*-sulfate. Optimal MS parameters were as follows: curtain gas 20 psi; nebulizer gas (GS1) and turbo gas (GS2) 40 psi; ion spray voltage 5500 V; source temperature 400 °C; collision energies was 45 eV and declustering potential was 40 V for both analytes. Due to the lack of blank bile matrix, calibration curves were plotted with corrected peak area ratios of DAPTAD-25OHD$_3$-3-*O*-sulfate and DAPTAD-d$_6$-25OHD$_3$-3-*O*-sulfate by subtracting "blank" samples without spiking with 25OHD$_3$-3-*O*-sulfate solution from the ones spiked with serial solutions.

Quantitation of DHEA-sulfate in recombinant SULT enzyme and human cytosol incubates

Incubation samples quenched with 50% acetonitrile were centrifuged at 12,000*g* for 5 min. The supernatant was transferred to a clean glass tube and the solvent removed under a nitrogen stream. The sample residues were reconstituted in mobile phase (30% acetonitrile in 5 mM ammonium acetate, pH 4.6) then subjected to LC/MS analysis using an Agilent MSD mass spectrometer coupled with an Agilent 1100 series LC system. Sample injection volumes were 20 μL on column and chromatographic separation of the analytes was achieved on a Symmetry C18 (2.1 mm × 150 mm, 3.5 μm) column (Waters, Milford, WA), with a mobile phase consisting of 5 mM ammonium acetate (A, pH 4.6) and acetonitrile (B) at 40 ºC. A linear gradient from 30% B

(0 – 2 min) to 50% B (11 – 11.5 min) over 15 min at 0.25 mL/min flow rate was employed. DHEA-sulfate and d_6-DHEA-sulfate eluted from the column at ~ 6.5 min. The mass spectrometer was operated in the negative ionization mode. The interface was maintained at 350 ^oC with a nitrogen nebulization pressure of 35 psi, resulting in a flow of 10 L/min. DHEA-sulfate and d_6-DHEA-sulfate were detected by selective ion monitoring at *m/z* 367 and 373, respectively, following 120 V ion fragmentation. Calibration standards were prepared in incubation buffer and processed as described for the incubation samples. Calibration curves were constructed by plotting the peak area ratios of DHEA-sulfate and d_6-DHEA-sulfate versus the corresponding DHEA-sulfate concentrations and fitting a linear regression equation to the data. Formation of DHEA-sulfate was then quantified by fitting the peak area ratios (metabolites/internal standard) from incubations to the calibration curve.

Hepatic RNA-Seq analysis

RNA Isolation. Human liver RNA was isolated from tissue samples and purified using a NucleoSpin® miRNA kit (Macherey-Nagel, Duren, Germany; Clonetech Labs, Mountain View, CA) according to manufacturer's protocol. Briefly, ~30 mg liver tissue was combined with 4 °C lysis buffer, homogenized using a TissueLyser LT (Qiagen, Valencia, CA), and allowed to sit at room temperature for 5 min. The solution was then added to the column. After centrifugation to bind the large RNA to the column, the column was treated with an rDNase solution at room temperature for at least 15 min. The flow-through containing the small RNA was treated, in order to precipitate out the protein. The small RNA was then bound to a new column. Following three wash steps of each column, the resulting large and small RNA were each eluted, quantitated and bioanalyzed for quality control using a Bioanalyzer 2100 (Agilent, Santa Clara, CA). Only RNA with RIN greater or equal to 7.0 was submitted for sequencing.

cDNA library preparation. Next-generation sequencing libraries were prepared from 1.25 µg of total RNA using the TruSeq Stranded mRNA kit (Illumina, San Diego, CA). All the steps required for sequence library construction have been automated and were performed on a Sciclone NGSx Workstation (Perkin Elmer, Waltham, MA). Ribosomal RNA was depleted by poly-A enrichment and first and second strand cDNA syntheses are performed. Each library was uniquely barcoded using the Illumina adapters and amplified using a total of 13 cycles of PCR. After amplification and cleanup, library concentrations are quantified using the Quant-it dsDNA Assay (Life Technologies, Carlsbad, CA). Libraries were normalized and pooled based on Agilent 2100 Bioanalyzer results (Agilent Technologies, Santa Clara, CA). Pooled libraries were size selected using a Pippin Prep (Sage Science, Beverly, MA) and then balanced by mass and pooled in batches of 96 with a final pool concentration of 2-3 nM for sequencing on the HiSeq 2500.

Read processing and final analysis pipeline. The read processing pipeline included the following steps: (1) base calls were generated in real-time on the HiSeq or NextSeq instrument; (2) Illumina RTA-generated BCL files were converted to FASTQ files; (3) custom scripts developed in-house were used to process the FASTQ files and to output de-multiplexed FASTQ files by lane and index sequence; (4) sequence read and base quality were checked using the FASTX-toolkit (http://hannonlab.cshl.edu/fastx_toolkit/) and FastQC (http://www.bioinformatics.babraham.ac.uk/projects/fastqc/); (5) sequences were aligned to hg19 with reference transcriptome Ensembl v67 using Tophat (Kim et al., 2013); and (6) custom scripts for quality assessment generate metrics. All aligned read data were subject to the following steps: (1) lane level bam data files were merged using the Picard MergeSamFiles tool and suspected PCR duplicates were marked, but not removed, in the alignment files using the

Picard MarkDuplicates tool (http://broadinstitute.github.io/picard/); (2) local realignment was performed around indels, and base quality score recalibration was run using GATK tools (McKenna et al., 2010); (3) variant detection was performed with the GATK Unified Genotyper version 2.6.5 (DePristo et al., 2011); (4) aligned data were used for isoform assembly and quantitation with Cufflinks (Kim et al., 2013; Trapnell et al., 2013); genomic features (e.g., *SULT2A1*) were quantitated with featureCounts (Liao et al., 2014); and (5) sample level QC scripts were executed to generate final sample level statistics. Differential expression analysis was performed concurrently with the Cufflinks suite of tools and DESeq (Anders and Huber, 2010).

DNA sequence analysis

DNA was isolated from liver samples, as described previously (Shirasaka et al., 2015), and candidate genes were sequenced using the PGRN-Seq platform developed for the Pharmacogenomics Research Network by Nickerson and colleagues (Gordon et al., 2016). For *SULT2A1*, sequence coverage included exons 1, 5, and 6, exon-intron boundaries, and parts of the 3' and 5' untranslated regions, which were all aligned to the hg19 human reference genome. Sequence data was filtered using VCFtools (Danecek et al., 2011). The average locus read depth was 155. All SNVs passed a Phred Quality score > 50, and for the SULT2A1 locus, the average Phred Quality score for all variant positions was 389,614. Single-nucleotide variants were annotated with SeattleSeq Annotation, briefly described by Ng et al. (Ng et al., 2009).

Quantitation of SULT2A1 and SULT1A1 proteins in hepatic cytosol

Sample preparation for SULT2A1, SULT1A1 and BSA protein quantification. BSA was used as a protein internal standard to address inter-sample and inter-day variability in the trypsin digestion whereas heavy labeled peptides were used as a control to address LC-MS/MS

instrument variability. 10 µL of BSA (100 µg total) was spiked into 80 µL of the liver cytosolic samples (2.0 mg/mL), and the protein mixture was denatured, reduced, alkylated as per published protocol (Prasad and Unadkat, 2014a; Prasad et al., 2016). Similarly, the denatured/alkylated protein was then desalted and precipitated using methanol:chloroform:water precipitation followed by re-suspension and digestion, as discussed before (Prasad et al., 2016). The digestion reaction was quenched by 20 µL of the labeled peptide internal standard cocktail containing the two heavy peptides listed in Supplementary Table 1S (prepared in 50% acetonitrile in water containing 0.1% formic acid) plus 10 µL of blank solvent (50% acetonitrile in water containing 0.1% formic acid). The samples were centrifuged at 5000*g* for 5 min at 4 °C, and 5 µL of the supernatants were injected onto the LC-MS/MS system.

LC-MS/MS peptide analysis. Surrogate peptides of SULT2A1, SULT1A1 and BSA were quantified using optimized LC-MS/MS parameters listed in Supplementary Tables 1 and 2 using AB Sciex 6500 tandem mass spectrometer (AB SCIEX, Ontario, Canada) coupled to Waters Acquity™ UPLC system (Waters, Hertfordshire, UK) with few modifications, mainly in the LC parameters. Briefly, a UPLC column (Acquity UPLC® HSS T3 1.8 µm, 2.1 × 100 mm, Waters) with a Security Guard column (C18, 4 mm × 2.0 mm) from Phenomenex (Torrance, CA) was eluted (0.3 mL/min) with a gradient mobile phase consisting of water and acetonitrile (with 0.1% formic acid; see below). The injection volume was 5 µL (~10 µg of total protein). The parent to product ion transitions for the analyte peptides and their respective SIL peptides were monitored using optimized LC-MS/MS parameters (Supplementary Tables 1 and 2) in ESI positive ionization mode. Peak areas of each fragment were calculated, multiple fragments of each peptide parent ion were averaged and the area ratios of light vs. heavy were calculated. Finally, SULT2A1 and SULT1A1 area ratios were normalized by the BSA ratios. Each sample was

analyzed twice on two different days and average of the two days was considered for the data analysis. For absolute quantification of SULT2A1 in the pooled cytosol sample, nine serial dilutions of the purified protein were digested and processed similar to the cytosol samples. The on-column amounts of SULT2A1 standard ranged from 0.15 fmol (lower limit of quantification, LLOQ) to 38 fmol.

Binding of 25OHD$_3$-3-*O*-sulfate and 25OHD$_3$ to the DBP

The binding assays were performed as described previously (Horst et al., 1981). Briefly, rat plasma was diluted 1/5000 (v/v) in 0.05 M phosphate buffer (pH 7.5) containing 0.01% gelatin and 0.01% merthiolate (PBG buffer). Each assay mixture was placed in a borosilicate glass tube and consisted of (1) 0.5 mL of 1/5000 dilution of vitamin D-deficient rat plasma in PBG buffer, (2) 6000-8000 cpm of [23,24-^{3}H]-25OHD$_3$ in 20 µL of 100% ethanol, and (3) vitamin D metabolites in 25 µL of ethanol. After 1-2 h incubation at 4 $^\circ$C, the bound vitamin D metabolites were separated from free by adding 0.2 mL of a mixture of cold 1.0% Norit A Charcoal and 0.1% Dextran T-70 in PBG buffer to each tube. After 30 min at 4 $^\circ$C, the tubes were spun at 1000 *g* for 10 min in a refrigerated centrifuge. A portion (0.5 mL) of the supernatant was removed for quantitation of the bound [^{3}H]-25OHD$_3$. The binding experiment was conducted with rat plasma so that we could directly compare new results to historical data generated by our lab using rat plasma (Wang et al., 2014). Previously, Bouillon et al. concluded that the heterogeneity between the genes encoding for DBP in rats and humans, and the subsequent structural difference between the two proteins, has no effect on their affinity or capacity to bind vitamin D metabolites (Bouillon et al., 1980).

Statistical analysis

All data are expressed as the mean ± standard deviation (S.D.) unless stated otherwise. Group comparisons were made using one-way ANOVA analysis with Dunnett's multiple comparison test. For all cell- and recombinant enzyme-based experiments, we used GraphPad Prism v.5 for the statistical analyses, and a p-value less than 0.05 was considered statistically significant. For results from experiments with human livers, we used a linear trend test (one-way ANOVA) to assess *SULT2A1* genotype-phenotype associations, and a p-value less than 0.05 ($p < 0.05$) was considered to be statistically significant. The regression coefficient, r^2, was calculated in Excel (Microsoft® Office Excel 2010, Microsoft Corporation, Redmond, WA).

A multivariate linear regression analysis of genetic, demographic and other variables for the liver donors was performed in R (version 3.3.3) to elucidate major determinants of interindividual variability in $25OHD_3$ sulfonation activity. Full details are given in the Supplementary Methods section. Regression analyses were performed with the log transformed activity data, because of its non-normal (skewed) distribution. A p-value less than 0.05 ($p < 0.05$) was considered to be statistically significant for all tests.

Results

Formation of $25OHD_3$-3-*O*-sulfate by human liver cytosols and recombinant SULTs

Sulfonation of $25OHD_3$ is catalyzed by cytosolic SULT isozymes. $25OHD_3$ contains two hydroxyl groups and presumably two different sulfate conjugate isomers either at the C-3 or C-25 positions could be produced (Figure 1A). Incubation of $25OHD_3$ with pooled human liver cytosols (HLC) and PAPS cofactor generated a single major sulfate product (retention time: 19.5 min) with selective mass ion monitoring at *m/z* 479, which corresponds to $[M - H]^-$ under the negative ion mode (Figure 1B). An identical peak was also detected with recombinant SULT2A1

and SULT1A1 incubations, but not SULT1B1, SULT1E1 and SULT2B1, under the incubation conditions that were employed. The activity of SULT2A1 greatly exceeded that of SULT1A1, which was seen in only one of three replicate experiments. The LC-MS characteristics of the predominant cytosolic metabolite were identical. Its LC retention time matched with that of the synthesized standard 25OHD$_3$-3-*O*-sulfate, indicating conjugation with a sulfate group at the C-3 position (Figure 1B). This was further confirmed by ion fragmentation pattern after PTAD derivation. As shown in Figure 1C, an identical daughter ion at *m/z* 378 indicated a direct conjugation at C-3 position and cleavage between C-6 and C-7, which is in agreement with the fragmentation pattern of standard 25OHD$_3$-3-*O*-sulfate. Based on this data, we conclude that the predominant product of SULT2A1 and human liver cytosol is 25OHD$_3$-3-*O*-sulfate. A minor peak (retention time: 20.0 min) with selective mass ion at *m/z* 479 was also observed in incubations with either SULT2A1 or HLC, however, whether this peak is 25OHD$_3$-25-*O*-sulfate or a 25OHD$_3$-3-*O*-sulfate stereoisomer remains unknown (Figure 1B).

Kinetic studies of 25OHD$_3$-3-*O*-sulfate formation were performed *in vitro* using pooled human liver cytosols, and recombinantly expressed SULT2A1 (Figure 2). The K_m and V_{max} values for 25OHD$_3$-3-*O*-sulfate formation estimated using a simple Michaelis-Menten kinetics model are presented in Table 1. Incubations with human liver cytosol and SULT2A1 yielded nearly identical mean apparent K_m values (3.43 vs 3.36 µM, respectively). In addition, when normalized to the measured specific SULT2A1 content (1360 ± 106 pmol/mg protein) of the pooled human liver cytosol used in these experiments, the mean V_{max} value was comparable to that of the pooled recombinant human SULT2A1 (17.7 and 21.3 pmol/min/nmol SULT2A1, respectively). The corresponding intrinsic sulfonation clearances were also similar – 5.15 and 6.59 µL/min/nmol SULT2A1, respectively. These results suggest that SULT2A1 is the

predominant source of sulfonation activity in human liver and could represent an important metabolic route for 25OHD$_3$ clearance.

25OHD$_3$-3-*O*-sulfate is the major metabolite formed from 25OHD$_3$ by human hepatocytes

Previous studies have demonstrated that at non-physiological concentrations (1 - 5 μM), 25OHD$_3$ is metabolized to 1α,25(OH)$_2$D$_3$, 24R,25(OH)$_2$D$_3$, 4α,25(OH)$_2$D$_3$, 4β,25(OH)$_2$D$_3$, 25OHD$_3$-3-*O*-glucuronide, 25OHD$_3$-25-*O*-glucuronide, and putative 5,6-*trans*-25OHD$_3$-25-*O*-glucuronide when incubated with human hepatocytes (Wang et al., 2014). However, formation of 25OHD$_3$-3-*O*-sulfate in human hepatocytes was not determined. For this investigation, a more physiological concentration of 25OHD$_3$ (50 nM) was applied to cultured human hepatocytes to generate a metabolite profile. As shown in Figure 3A, all major metabolites of 25OHD$_3$, except 1α,25(OH)$_2$D$_3$, were detected in the incubations. 25OHD$_3$-3-*O*-sulfate was the most abundant product observed, followed by 24R,25(OH)$_2$D$_3$, 4,25(OH)$_2$D$_3$ [4α,25(OH)$_2$D$_3$ & 4β,25(OH)$_2$D$_3$], and 25OHD$_3$-glucuronides. Formation of these 25OHD$_3$ metabolites occurred in a linear, time-dependent manner, except for 4β,25(OH)$_2$D$_3$ and 4α,25(OH)$_2$D$_3$ formation, which underwent extensive sequential glucuronidation, as previously reported (Wang et al., 2013a).

By comparison, renal tubule epithelial cells and LS180 intestinal epithelial cells showed no detectable formation of 25OHD$_3$-3-*O*-sulfate during a 24-hour incubation with 50 nM 25OHD$_3$ (data not shown). These cells have previously been shown to catalyze the 24-hydroxylation of 25OHD$_3$ under similar culture conditions (Zheng et al., 2012; Weber et al., 2016). Based on the assay limit of detection, culture conditions and the approximate number of cells per well, it was estimated that 25OHD$_3$ sulfonation activity per renal tubule epithelial cell or LS180 cell was < 10% that of cryopreserved human hepatocytes.

Chronic exposure to pregnane X receptor (PXR) agonists, such as rifampicin, can cause a reduction in plasma $25OHD_3$ blood levels (Brodie et al., 1980) by a mechanism that is not completely understood. In a previous study, we showed that treatment of human hepatocytes with rifampicin significantly increased the $25OHD_3$ 4-hydroxylation pathway by induction of hepatic CYP3A4 (Wang et al., 2013a). The effect of rifampicin on $25OHD_3$ sulfonation is unclear (Echchgadda et al., 2007; Fang et al., 2007) and, thus, was explored. After incubation of hepatocytes with 10 µM rifampicin or vehicle (0.1% DMSO) for 48 hours, the cells were washed and incubated with 50 nM $25OHD_3$ for 2, 4, 8 and 24 hours. There was no apparent difference in $25OHD_3$-3-*O*-sulfate formation between rifampicin-treated and control hepatocytes, whereas as expected, $4,25(OH)_2D_3$ formation was significantly (37.6% after 24 hr) induced by rifampicin treatment (Figure 3B).

Associations between *SULT2A1* gene variants and hepatic SULT2A1 mRNA and protein abundances and cytosolic sulfonation activities

With the identification of SULT2A1 as the principal catalyst of $25OHD_3$-3-*O*-sulfate formation, we sought to test whether variation in the *SULT2A1* gene sequence might contribute to interindividual differences in hepatic sulfonation activity. To that end, we accessed pre-existing sequence data (Gordon et al., 2016) for parts of the *SULT2A1* gene (coverage included exons 1, 5 and 6, intron-exon boundaries, and parts of the 3' and 5' untranslated regions) in DNA isolated from 258 human livers. Relative to the reference human genome, a total of 12 different SNVs (single nucleotide variant) were identified; 8 in untranslated regions, 1 intronic, 1 synonymous coding, and 2 nonsynonymous coding variant (Supplemental Figure 1). Of these, 8 SNVs had minor allele frequencies > 0.6%. Three variants were common (rs296366, T>C; rs296365, C>G; and rs296361, G>A) and detected at an allele frequency of 80%, 27% and 15%,

respectively, and all were in Hardy-Weinberg equilibrium. Of the three common SNVs, two (rs296366, rs296365) were located in the 3'-region of the gene and one was near the intron-1/exon-1 boundary (rs296361). All three exhibited a high degree of linkage disequilibrium (not shown). An assessment of SULT2A1 mRNA content of the same livers was obtained by RNA-Seq analysis and revealed significant associations between rs296361, but not rs296366, rs296365, and the relative level of hepatic SULT2A1 mRNA content, with a 70% lower mean level of mRNA in livers homozygous for the rs296361 A allele, compared to the reference G allele (Supplemental Figure 2). Accordingly, we focused further analysis on rs296361 because of its association with mRNA level and potential of the intron-1 SNV to disrupt mRNA splicing and message accumulation.

Cytosol isolated from the same bank of human livers was subjected to quantitative analysis of SULT2A1 protein content and $25OHD_3$ sulfonation activity at a substrate concentration of 5 µM. There were significant associations between *SULT2A1* rs296361 and total SULT2A1 protein (Figure 4A) and the cytosolic $25OHD_3$-3-*O*-sulfate formation rate (Figure 4B). Consistent with the mRNA and protein results, the mean rate of $25OHD_3$-3-*O*-sulfate formation in cytosol from livers homozygous for the variant allele was only 30% of that found for the livers homozygous for the reference allele. Not surprisingly, there was a statistically significant correlation between SULT2A1 protein content and the $25OHD_3$-3-*O*-sulfate formation rate, where differences in the protein level explained 22% of the unadjusted variance in sulfonation activity (Figure 5A).

Correlation between $25OHD_3$-3-*O*-sulfate formation and DHEA-sulfate formation by human liver cytosol

DHEA is considered to be a selective probe substrate for SULT2A1 (Mueller et al., 2015) and, thus, we determined the rate of formation of DHEA-3-*O*-sulfate in liver cytosolic preparations incubated with 5 µM µM DHEA. As seen in Supplemental Figure 3, there was a significant association between the *SULT2A1* rs296361 variant and the DHEA-3-*O*-sulfate formation rate, which was also strongly correlated with cytosolic SULT2A1 protein content; r^2 = 0.71 (Supplemental Figure 4). There was also a significant correlation between the rates of 25OHD$_3$-3-*O*-sulfate and DHEA-3-*O*-sulfate formation among the panel of human livers tested, $r^2 = 0.27$, $p < 0.0001$ (Figure 5B), indicative of a common enzyme catalyzing the two reactions. However, an examination of the 25OHD$_3$ sulfonation rate regression curves suggested the possibility of a second enzyme contributing to 25OHD$_3$-3-*O*-sulfate formation at the substrate concentration tested. Because we had observed some activity with the recombinantly expressed SULT1A1 enzyme, we quantified SULT1A1 protein levels in the panel of human liver cytosols. There was no association between cytosolic SULT1A1 protein content and 25OHD$_3$-3-*O*-sulfate formation rate (data not shown).

Stratification of the 25OHD$_3$ sulfonation activity by the liver bank source revealed higher average sulfonation activity in the UW livers, compared to the St Jude livers (data not shown). This was not the case for DHEA sulfonation activity. A multivariate analysis that considered *SULT2A1* genotype and donor sex, age, ethnicity, liver repository (SJLB or UWLB), duration of tissue storage at -80°C as covariates, revealed significant contributions from SULT2A1 rs296361 genotype, liver repository and storage duration to the variance in the log 25OHD$_3$-3-*O*-sulfate formation rate (Table 2). The full regression model explained 47% of the variance in the log 25OHD$_3$ sulfonation rate.

Detection of 25OHD$_3$-3-*O*-sulfate in pooled human plasma, bile and urine

The presence or absence of 25OHD$_3$-3-*O*-sulfate in human plasma, bile and urine was evaluated. Due to the complexity of these biological matrices, an optimized extraction method was developed and employed to partially purify the bio-samples individually. An anion exchange cartridge was used to extract 25OHD$_3$-3-*O*-sulfate from plasma, bile and urine samples. Deuterium labeled sulfate standard was applied to identify potential sulfate peak and used to estimate and then correct for the total recovery during solid-phase extraction and subsequent steps. As shown in Figure 6A, a representative chromatogram derived from plasma extracts clearly showed the presence of 25OHD$_3$-3-*O*-sulfate in human plasma. An analysis of plasma from 21 healthy adults produced mean concentrations of 130.8 ± 70.8, 96.0 ± 44.0, 12.0 ± 7.7, and 0.26 ± 0.14 nM for 25OHD$_3$, 25OHD$_3$-3-*O*-sulfate, 24R,25(OH)$_2$D$_3$ and 4β,25(OH)$_2$D$_3$, respectively.

The presence of 25OHD$_3$-3-*O*-sulfate in human bile was suggested by detection after solid-phase extraction of a peak with a mass ion of *m/z* 479, which corresponds to $[M - H]^-$ under the negative ion mode, that co-eluted with standard 25OHD$_3$-3-*O*-sulfate (Figure 6A). Reacting the solid-phase extract with the vitamin D derivatizing agent, PTAD, resulted in a loss of the ion at *m/z* 479 (data not shown). To confirm this finding, we reacted the extracted material with another derivatizing reagent, DAPTAD, which provided greater analytical sensitivity. As seen in Figure 6B, a single product co-eluting with the derivatized deuterated internal standard was observed. Comparing the signal to that of reference 25OHD$_3$-3-*O*-sulfate standards yielded an estimated pooled bile concentration of 2.55 nM (mean of two replicate determinations).

25OHD$_3$-3-*O*-sulfate was not detected in 0.5 mL human urine (n = 3) under underivatized or derivatized conditions.

Binding of 25OHD$_3$-3-*O*-sulfate to rat plasma DBP

The presence of 25OHD$_3$-3-*O*-sulfate in plasma, but not urine, suggested the possibility that it might have significant binding affinity for the DBP, restricting its excretion by the kidney, as occurs for 25OHD$_3$. Previous studies have shown that 25OHD$_3$-3-*O*-glucuronide, but not 25OHD$_3$-25-*O*-glucuronide, binds tightly to DBP (Wang et al., 2014). Due to the structure similarity, we surmised that 25OHD$_3$-3-*O*-sulfate could also bind to DBP. To test this hypothesis, the concentration-dependent binding of 25OHD$_3$-3-*O*-sulfate, 25OHD$_3$-3-*O*-glucuronide, and 25OHD$_3$ to rat plasma DBP was measured by radio-ligand binding assay (Horst et al., 1981). As seen in Figure 7, the binding affinity of 25OHD$_3$-3-*O*-sulfate for DBP was essentially identical to that of 25OHD$_3$ and 25OHD$_3$-3-*O*-glucuronide. The mean EC_{50} for 25OHD$_3$, 25OHD$_3$-3-*O*-glucruonide, and 25OHD$_3$-3-*O*-sulfate binding to DBP under current incubation conditions were 0.82, 0.74, and 0.72 pmol, respectively.

Discussion

Previous studies from our research group demonstrated that glucuronidation of 25OHD$_3$ occurs in humans and is catalyzed primarily by UGT1A3 and UGT1A4 (Wang et al., 2014). Herein, we confirm that 25OHD$_3$-3-*O*-sulfate is also a quantitatively important circulating product of 25OHD$_3$ (Axelson, 1985; Shimada et al., 1995) and report for the first time that it is generated primarily in the liver by the enzyme SULT2A1. The sulfate conjugate was the dominant metabolic product of 25OHD$_3$ produced by primary human hepatocytes when incubated with a physiologically relevant 50 nM concentration of 25OHD$_3$. Thus, inter-individual differences in sulfonation activity may be a major source of variation in circulating blood 25OHD$_3$ concentrations, assuming that hepatic clearance of 25OHD$_3$ is an important determinant of 25OHD$_3$ accumulation in the body.

Results from our kinetic experiments, revealing comparable K_m and V_{max} values when normalized for SULT2A1 content, suggest that this isozyme is the predominant catalyst of the 25OHD$_3$ sulfonation reaction in human liver. This conclusion is supported in part by the positive regression of liver cytosolic sulfonation activity against SULT2A1 protein content and the strong association between *SULT2A1* genetic variation and liver cytosolic sulfonation activity. However, we note that approximately one-half of the variance in liver cytosolic 25OHD$_3$ sulfonation activity remained unexplained and that variation in cytosolic SULT2A1 protein content explained only 21% of the unadjusted metabolic activity towards this substrate, in contrast to a much stronger correlation between cytosolic DHEA sulfonation activity and SULT2A1 protein content. Non-specific factors associated with the liver procurement site explained a substantial fraction of the observed variance in liver cytosolic 25OHD$_3$ sulfonation activity and variable storage time and possible loss of activity but not measured protein was also contributory (Table 2). We speculate that these and possibly other factors (e.g., uncontrolled substrate-selective protein-SULT2A1 interactions) masked what would otherwise have been a stronger association between SULT2A1 protein level and sulfonation activity.

SULT2A1 is known to metabolize hydroxysteroids, such as estradiol, DHEA and bile acids (Chatterjee et al., 2005). That it also catalyzes 25OHD$_3$ sulfonation is not surprising, considering structural similarities. The regiospecificity of SULT2A1 towards 25OHD$_3$ sulfonation, almost exclusively at the 3-position, is similar to that observed for hydroxysteroids and oxysterols. Interestingly, the related SULT isoform, SULT2B1, showed little activity towards 25OHD$_3$, which is in contrast to its ability to generate sulfate metabolites of hydroxysteroids and oxysterols that are substrates for SULT2A1 (Falany and Rohn-Glowacki, 2013). SULT2B1 is expressed primarily in extra-hepatic tissues (Falany and Rohn-Glowacki,

2013), whereas SULT2A1 is highly expressed in the liver and adrenal cortex and less so in the gastrointestinal tract (Chatterjee et al., 2005). This distribution pattern suggests that there will be limited $25OHD_3$ sulfonation activity outside of the liver. Consistent with these findings, no detectable $25OHD_3$ sulfonation was observed in either human intestinal LS180 cells or renal epithelial cells incubated with a physiologically-relevant concentration of $25OHD_3$.

We found no evidence that hepatic $25OHD_3$ sulfonation activity is induced by PXR agonists, based on our negative results with rifampicin and primary human hepatocytes, further supporting a role for enhanced oxidative metabolism in the reduction of plasma $25OHD_3$ levels following chronic rifampicin treatment (Brodie et al., 1980). This result is concordant with the findings of Fang et al (Fang et al., 2007) who reported inconsistent inductive responses in a relatively large number of primary human hepatocyte preparations and, with additional experiments, suggested that PXR actually represses SULT2A1 expression and that sporadic inductive responses in hepatocyte are mediated by a non-PXR mechanism. However, it is at odds with other published results from PXR-transfected Caco-2 and HepG2 systems that suggest transcriptional enhancement of SULT2A1 by PXR agonists (Echchgadda et al., 2007). Characterization of $25OHD_3$-3-*O*-sulfate levels following rifampicin treatment *in vivo* could help clarify the discrepancy. It is noteworthy that SULT2A1 is thought to be regulated by $1\alpha,25(OH)_2D_3$ (Echchgadda et al., 2004), suggesting an auto-feedback mechanism of vitamin D regulation, as described for CYP24 (Haussler et al., 2013) and proposed for CYP3A4 (Xu et al., 2006; Wang et al., 2013a).

Partial sequence analysis of the *SULT2A1* gene revealed a strong association between a single nucleotide variant (rs296361) and cytosolic sulfonation activity and SULT2A1 protein abundance. Accordingly, we hypothesize that this *SULT2A1* SNV may contribute to inter-

individual differences in the circulating plasma 25OHD$_3$-3-*O*-sulfate and 25OHD$_3$ levels, something that should be tested in future investigations. The minor allele frequency for rs296361, as reported in dbSNP (NCBI), is 16.1%, 0.4%, 0.3%, 6.2% and 10.6% for European, East Asian, African, Admixed American and South Asian, respectively. Interestingly, although the variant SNV resides within intron-1, it was also strongly associated with hepatic *SULT2A1* mRNA abundance, suggesting that RNA splicing or the accumulation of the mature message is somehow affected. RNA-Seq analysis did not reveal alternative splice variants, suggesting that the efficiency of splicing was altered by the SNV, perhaps by altering the function of a splice enhancer or repressor sequence. It is also possible that the intron-1 SNV is in linkage disequilibrium with another allelic variant not detected by our sequencing analysis (e.g., in unsequenced exonic and intronic regions or an upstream or downstream regulatory region of the *SULT2A1* gene) and that rs296361 has no causal effect on the SULT2A1 phenotype. It is important to note that a copy number variation (CNV) in the SULT2A1 gene locus has also been described (Ekstrom and Rane, 2015) and has been associated with the urinary excretion of DHEA-sulfate and testosterone-sulfate (Schulze et al., 2013). However, the frequency of the CNV appears to be much lower that that of rs296361. Whether or not there is linkage disequilibrium between the two gene variants remains to be determined, as we did not test for the CNV with the sequencing platform that we employed. Regardless of the mechanism behind the rs296361 – SULT2A1 phenotype associations, the data strongly suggest that this common genetic variation could influence the biological effects of 25OHD$_3$, DHEA, and other important hormone signaling molecules metabolized by SULT2A1.

25OHD$_3$-3-*O*-sulfate was found to have a high binding affinity for DBP, which explains its relatively high abundance in plasma and absence from urine. The crystal structure of DBP

DMD Fast Forward. Published on January 17, 2018 as DOI: 10.1124/dmd.117.078428
This article has not been copyedited and formatted. The final version may differ from this version.

indicates that the vitamin D-binding site is a cleft, which can easily accommodate large substituents at the C-3 position of $25OHD_3$, such as conjugated moieties (Verboven et al., 2002). High binding affinity to DBP would reduce the renal excretion of $25OHD_3$-3-*O*-sulfate into urine. We speculate that the complex of $25OHD_3$-3-*O*-sulfate and DBP is filtered and then re-absorbed in renal proximal tubules by megalin/cubilin mediated endocytosis, as shown for the $25OHD_3$-DBP complex (Rowling et al., 2006).

Although $25OHD_3$-3-*O*-sulfate is a major circulating form of vitamin D_3, whether it possesses biological activity directly or indirectly is unclear. A number of studies have been conducted to understand the biological activities of vitamin D_3-sulfate, a conjugated metabolite of vitamin D_3 (Higaki et al., 1965; Sahashi et al., 1967a; Sahashi et al., 1967b; Sahashi et al., 1969). Vitamin D_3-sulfate was synthesized previously (Reeve et al., 1981) and its biological activity was determined in a vitamin D-deficient rat model. Activity was observed, but only at doses higher than what can be elicited by vitamin D_3 (Nagubandi et al., 1981). Later studies also showed less biological activity of vitamin D_3-sulfate than free vitamin D_3 *in vivo* (Cancela et al., 1985). However, in each of these studies, vitamin D_3-sulfate was administered, rather than having the metabolite generated *in situ*, with the uncertainties of bioavailability and access to cellular sites that complicate quantitative comparisons. Thus, it is possible that $25OHD_3$-3-*O*-sulfate might undergo hydrolysis, catalyzed by ubiquitous sulfatases and regenerate $25OHD_3$. This type of hormone conjugate cycling is observed for estrogen and DHEA (Mueller et al., 2015), where the sulfo-conjugates are the dominant form in blood circulation and are distributed to peripheral tissues where de-sulfonation can occur. In the case of DHEA-3-*O*-sulfate, conversion to DHEA is followed by metabolism to androstenedione and downstream androgens and estrogens (Strott, 2002).

Finally, given the detection of 25OHD$_3$-3-*O*-sulfate in bile, we are intrigued by the possibility that preferential delivery of the hormone conjugate to the duodenum and upper small intestine might explain the preferential expression of vitamin D receptor target genes, such as CYP3A4, TRPV6 and calbindin D9K, in the upper small intestine (Wang et al., 2013b). Results from unpublished studies indicate that 25OHD$_3$-3-*O*-sulfate is a substrate for the cell uptake transporter, OATP2B1, which is expressed in the intestinal epithelia (Drozdzik et al., 2014). Once absorbed into mucosal epithelial cells, 25OHD$_3$-3-*O*-sulfate could be hydrolyzed to 25OHD$_3$ and then undergo 1α-hydroxylation to the active hormone and contribute to the regulation of TPRV6, calbindin D9K and CYP3A4 (Wang et al., 2013b). With regard to the kidney, 25OHD$_3$-3-*O*-sulfate bound to the DBP in blood could be filtered in the glomerulus and then reabsorbed in the proximal tubular epithelium through the action of megalin/cubulin, similar to what occurs for the 25OHD$_3$-DBP complex (Negri, 2006). Again, intracellular hydrolysis of the conjugate and bioactivation to 1α,25(OH)$_2$D$_3$ could contribute to the known biological effects of vitamin D in this tissue. Further work is needed to explore these mechanistic hypotheses.

Acknowledgements

We thank Professor Dr. Evan D. Kharasch at the Washington University in St. Louis, USA for generously providing human bile. We also thank Dr. Nicholas J. Koszewski, and Dr. Jesse P. Goff at the Iowa State University for helping on the vitamin D binding protein competitive assay.

Authorship Contributions

Participated in research design: Wong, Wang, Foti, Prasad, Chaudhry, Schuetz, Horst, Mao, de Boer, Thummel

Conducted experiments: Wong, Wang, B. Chapron, Suzuki, Claw, Gao, Foti, Prasad, A. Chapron, Calamia, Horst

Contributed new reagents or analytical tools: Foti, Schuetz

Performed data analysis: Wong, Wang, B. Chapron, Suzuki, Claw, Gao, Foti, Prasad, A. Chapron, Calamia, Chaudhry, Schuetz, Horst, Mao, Thornton, Thummel

Wrote or contributed to the writing of the manuscript: Wong, Wang, B. Chapron, Suzuki, Claw, Gao, Foti, Prasad, A. Chapron, Calamia, Chaudhry, Schuetz, Horst, Mao, de Boer, Thornton, Thummel

References

Ahn J, Yu K, Stolzenberg-Solomon R, Simon KC, McCullough ML, Gallicchio L, Jacobs EJ, Ascherio A, Helzlsouer K, Jacobs KB, Li Q, Weinstein SJ, Purdue M, Virtamo J, Horst R, Wheeler W, Chanock S, Hunter DJ, Hayes RB, Kraft P, and Albanes D (2010) Genome-wide association study of circulating vitamin D levels. *Hum Mol Genet* **19:**2739-2745.

Anders S and Huber W (2010) Differential expression analysis for sequence count data. *Genome Biol* **11:**R106.

Arguelles LM, Langman CB, Ariza AJ, Ali FN, Dilley K, Price H, Liu X, Zhang S, Hong X, Wang B, Xing H, Li Z, Liu X, Zhang W, Xu X, and Wang X (2009) Heritability and environmental factors affecting vitamin D status in rural Chinese adolescent twins. *J Clin Endocrinol Metab* **94:**3273-3281.

Axelson M (1985) 25-Hydroxyvitamin D3 3-sulphate is a major circulating form of vitamin D in man. *FEBS Lett* **191:**171-175.

Axelson M (1987) The cholecalciferol sulphate system in mammals. *J Steroid Biochem* **26:**369-373.

Banerjee N, Fonge H, Mikhail A, Reilly RM, Bendayan R, and Allen C (2013) Estrone-3-sulphate, a potential novel ligand for targeting breast cancers. *PLoS One* **8:**e64069.

Berry D and Hypponen E (2011) Determinants of vitamin D status: focus on genetic variations. *Curr Opin Nephrol Hypertens* **20:**331-336.

Bouillon R, van Baelen H, and de Moor P (1980) Comparative study of the affinity of the serum vitamin D-binding protein. *J Steroid Biochem* **13:**1029-1034.

Brodie MJ, Boobis AR, Dollery CT, Hillyard CJ, Brown DJ, MacIntyre I, and Park BK (1980) Rifampicin and vitamin D metabolism. *Clin Pharmacol Ther* **27:**810-814.

Bu FX, Armas L, Lappe J, Zhou Y, Gao G, Wang HW, Recker R, and Zhao LJ (2010) Comprehensive association analysis of nine candidate genes with serum 25-hydroxy vitamin D levels among healthy Caucasian subjects. *Hum Genet* **128:**549-556.

Cancela L, Marie PJ, Le Boulch N, and Miravet L (1985) Vitamin D3 3 beta sulfate has less biological activity than free vitamin D3 during pregnancy in rats. *Biol Neonate* **48:**274-284.

Chatterjee B, Echchgadda I, and Song CS (2005) Vitamin D receptor regulation of the steroid/bile acid sulfotransferase SULT2A1. *Methods Enzymol* **400:**165-191.

Danecek P, Auton A, Abecasis G, Albers CA, Banks E, DePristo MA, Handsaker RE, Lunter G, Marth GT, Sherry ST, McVean G, Durbin R, and Genomes Project Analysis G (2011) The variant call format and VCFtools. *Bioinformatics* **27:**2156-2158.

DeLuca HF (1988) The vitamin D story: a collaborative effort of basic science and clinical medicine. *FASEB J* **2:**224-236.

DePristo MA, Banks E, Poplin R, Garimella KV, Maguire JR, Hartl C, Philippakis AA, del Angel G, Rivas MA, Hanna M, McKenna A, Fennell TJ, Kernytsky AM, Sivachenko AY, Cibulskis K, Gabriel SB, Altshuler D, and Daly MJ (2011) A framework for variation discovery and genotyping using next-generation DNA sequencing data. *Nat Genet* **43:**491-498.

Drozdzik M, Groer C, Penski J, Lapczuk J, Ostrowski M, Lai Y, Prasad B, Unadkat JD, Siegmund W, and Oswald S (2014) Protein abundance of clinically relevant multidrug transporters along the entire length of the human intestine. *Mol Pharm* **11:**3547-3555.

Echchgadda I, Song CS, Oh T, Ahmed M, De La Cruz IJ, and Chatterjee B (2007) The xenobiotic-sensing nuclear receptors pregnane X receptor, constitutive androstane

receptor, and orphan nuclear receptor hepatocyte nuclear factor 4alpha in the regulation of human steroid-/bile acid-sulfotransferase. *Mol Endocrinol* **21:**2099-2111.

Echchgadda I, Song CS, Roy AK, and Chatterjee B (2004) Dehydroepiandrosterone sulfotransferase is a target for transcriptional induction by the vitamin D receptor. *Mol Pharmacol* **65:**720-729.

Ekstrom L and Rane A (2015) Genetic variation, expression and ontogeny of sulfotransferase SULT2A1 in humans. *Pharmacogenomics J* **15:**293-297.

Falany CN and Rohn-Glowacki KJ (2013) SULT2B1: unique properties and characteristics of a hydroxysteroid sulfotransferase family. *Drug Metab Rev* **45:**388-400.

Fang HL, Strom SC, Ellis E, Duanmu Z, Fu J, Duniec-Dmuchowski Z, Falany CN, Falany JL, Kocarek TA, and Runge-Morris M (2007) Positive and negative regulation of human hepatic hydroxysteroid sulfotransferase (SULT2A1) gene transcription by rifampicin: roles of hepatocyte nuclear factor 4alpha and pregnane X receptor. *J Pharmacol Exp Ther* **323:**586-598.

Fuleihan Gel H, Bouillon R, Clarke B, Chakhtoura M, Cooper C, McClung M, and Singh RJ (2015) Serum 25-Hydroxyvitamin D Levels: Variability, Knowledge Gaps, and the Concept of a Desirable Range. *J Bone Miner Res* **30:**1119-1133.

Gao C, Bergagnini-Kolev MC, Liao MZ, Wang Z, Wong T, Calamia JC, Lin YS, Mao Q, and Thummel KE (2017) Simultaneous quantification of 25-hydroxyvitamin D3-3-sulfate and 25-hydroxyvitamin D3-3-glucuronide in human serum and plasma using liquid chromatography-tandem mass spectrometry coupled with DAPTAD-derivatization. *J Chromatogr B Analyt Technol Biomed Life Sci* **1060:**158-165.

Gordon AS, Fulton RS, Qin X, Mardis ER, Nickerson DA, and Scherer S (2016) PGRNseq: a targeted capture sequencing panel for pharmacogenetic research and implementation. *Pharmacogenet Genomics* **26:**161-168.

Haussler MR, Whitfield GK, Kaneko I, Haussler CA, Hsieh D, Hsieh JC, and Jurutka PW (2013) Molecular mechanisms of vitamin D action. *Calcif Tissue Int* **92:**77-98.

Higaki M, Takahashi M, Suzuki T, and Sahashi Y (1965) Metabolic activities of vitamin D in animals. 3. Biogenesis of vitamin D sulfate in animal tissues. *J Vitaminol (Kyoto)* **11:**261-265.

Higashi T, Goto A, Morohashi M, Ogawa S, Komatsu K, Sugiura T, Fukuoka T, and Mitamura K (2014) Development and validation of a method for determination of plasma 25-hydroxyvitamin D3 3-sulfate using liquid chromatography/tandem mass spectrometry. *J Chromatogr B Analyt Technol Biomed Life Sci* **969:**230-234.

Higashi T, Shimada K, and Toyo'oka T (2010) Advances in determination of vitamin D related compounds in biological samples using liquid chromatography-mass spectrometry: a review. *J Chromatogr B Analyt Technol Biomed Life Sci* **878:**1654-1661.

Holick MF (2007) Vitamin D deficiency. *N Engl J Med* **357:**266-281.

Holick MF, Binkley NC, Bischoff-Ferrari HA, Gordon CM, Hanley DA, Heaney RP, Murad MH, Weaver CM, and Endocrine S (2011) Evaluation, treatment, and prevention of vitamin D deficiency: an Endocrine Society clinical practice guideline. *J Clin Endocrinol Metab* **96:**1911-1930.

Horst RL, Reinhardt TA, Beitz DC, and Littledike ET (1981) A sensitive competitive protein binding assay for vitamin D in plasma. *Steroids* **37:**581-591.

Hossein-nezhad A and Holick MF (2013) Vitamin D for health: a global perspective. *Mayo Clin Proc* **88:**720-755.

Hunter D, De Lange M, Snieder H, MacGregor AJ, Swaminathan R, Thakker RV, and Spector TD (2001) Genetic contribution to bone metabolism, calcium excretion, and vitamin D and parathyroid hormone regulation. *J Bone Miner Res* **16:**371-378.

Jones G, Prosser DE, and Kaufmann M (2014) Cytochrome P450-mediated metabolism of vitamin D. *J Lipid Res* **55:**13-31.

Kim D, Pertea G, Trapnell C, Pimentel H, Kelley R, and Salzberg SL (2013) TopHat2: accurate alignment of transcriptomes in the presence of insertions, deletions and gene fusions. *Genome Biol* **14:**R36.

Liao Y, Smyth GK, and Shi W (2014) featureCounts: an efficient general purpose program for assigning sequence reads to genomic features. *Bioinformatics* **30:**923-930.

McKenna A, Hanna M, Banks E, Sivachenko A, Cibulskis K, Kernytsky A, Garimella K, Altshuler D, Gabriel S, Daly M, and DePristo MA (2010) The Genome Analysis Toolkit: a MapReduce framework for analyzing next-generation DNA sequencing data. *Genome Res* **20:**1297-1303.

Mueller JW, Gilligan LC, Idkowiak J, Arlt W, and Foster PA (2015) The Regulation of Steroid Action by Sulfation and Desulfation. *Endocr Rev* **36:**526-563.

Nagubandi S, Londowski JM, Bollman S, Tietz P, and Kumar R (1981) Synthesis and biological activity of vitamin D3 3 beta-sulfate. Role of vitamin D3 sulfates in calcium homeostasis. *J Biol Chem* **256:**5536-5539.

Negri AL (2006) Proximal tubule endocytic apparatus as the specific renal uptake mechanism for vitamin D-binding protein/25-(OH)D3 complex. *Nephrology (Carlton)* **11:**510-515.

Ng SB, Turner EH, Robertson PD, Flygare SD, Bigham AW, Lee C, Shaffer T, Wong M, Bhattacharjee A, Eichler EE, Bamshad M, Nickerson DA, and Shendure J (2009) Targeted capture and massively parallel sequencing of 12 human exomes. *Nature* **461:**272-276.

Ogawa S, Ooki S, Morohashi M, Yamagata K, and Higashi T (2013) A novel Cookson-type reagent for enhancing sensitivity and specificity in assessment of infant vitamin D status using liquid chromatography/tandem mass spectrometry. *Rapid Commun Mass Spectrom* **27:**2453-2460.

Prasad B, Gaedigk A, Vrana M, Gaedigk R, Leeder JS, Salphati L, Chu X, Xiao G, Hop C, Evers R, Gan L, and Unadkat JD (2016) Ontogeny of Hepatic Drug Transporters as Quantified by LC-MS/MS Proteomics. *Clin Pharmacol Ther* **100:**362-370.

Prasad B and Unadkat JD (2014a) Comparison of Heavy Labeled (SIL) Peptide versus SILAC Protein Internal Standards for LC-MS/MS Quantification of Hepatic Drug Transporters. *Int J Proteomics* **2014:**451510.

Prasad B and Unadkat JD (2014b) Optimized approaches for quantification of drug transporters in tissues and cells by MRM proteomics. *AAPS J* **16:**634-648.

Reeve LE, DeLuca HF, and Schnoes HK (1981) Synthesis and biological activity of vitamin D3-sulfate. *J Biol Chem* **256:**823-826.

Rowling MJ, Kemmis CM, Taffany DA, and Welsh J (2006) Megalin-mediated endocytosis of vitamin D binding protein correlates with 25-hydroxycholecalciferol actions in human mammary cells. *J Nutr* **136:**2754-2759.

Sahashi Y, Suzuki T, Higaki M, and Asano T (1967a) Metabolism of vitamin D in animals. V. Isolation of vitamin D sulfate from mammalian milk. *J Vitaminol (Kyoto)* **13:**33-36.

Sahashi Y, Suzuki T, Higaki M, and Asano T (1969) Antirachitic potency of vitamin D sulfate in human milk. *J Vitaminol (Kyoto)* **15:**78-82.

Sahashi Y, Suzuki T, Higaki M, Takahashi M, and Asano T (1967b) Metabolic activities of vitamin D in animals. VI. Physiological activities of vitamin D sulfate. *J Vitaminol (Kyoto)* **13:**37-40.

Sanchez-Guijo A, Oji V, Hartmann MF, Traupe H, and Wudy SA (2015) Simultaneous quantification of cholesterol sulfate, androgen sulfates, and progestagen sulfates in human serum by LC-MS/MS. *J Lipid Res* **56:**1843-1851.

Schulze J, Johansson M, Thorngren JO, Garle M, Rane A, and Ekstrom L (2013) SULT2A1 Gene Copy Number Variation is Associated with Urinary Excretion Rate of Steroid Sulfates. *Front Endocrinol (Lausanne)* **4:**88.

Shea MK, Benjamin EJ, Dupuis J, Massaro JM, Jacques PF, D'Agostino RB, Sr., Ordovas JM, O'Donnell CJ, Dawson-Hughes B, Vasan RS, and Booth SL (2009) Genetic and non-genetic correlates of vitamins K and D. *Eur J Clin Nutr* **63:**458-464.

Shimada K, Mitamura K, and Kitama N (1995) Quantitative determination of 25-hydroxyvitamin D3 3-sulphate in human plasma using high performance liquid chromatography. *Biomed Chromatogr* **9:**229-232.

Shirasaka Y, Chaudhry AS, McDonald M, Prasad B, Wong T, Calamia JC, Fohner A, Thornton TA, Isoherranen N, Unadkat JD, Rettie AE, Schuetz EG, and Thummel KE (2015) Interindividual variability of CYP2C19-catalyzed drug metabolism due to differences in gene diplotypes and cytochrome P450 oxidoreductase content. *Pharmacogenomics J* **16:**375-387.

Strott CA (2002) Sulfonation and molecular action. *Endocr Rev* **23:**703-732.

Theodoratou E, Tzoulaki I, Zgaga L, and Ioannidis JP (2014) Vitamin D and multiple health outcomes: umbrella review of systematic reviews and meta-analyses of observational studies and randomised trials. *BMJ* **348:**g2035.

Trapnell C, Hendrickson DG, Sauvageau M, Goff L, Rinn JL, and Pachter L (2013) Differential analysis of gene regulation at transcript resolution with RNA-seq. *Nat Biotechnol* **31:**46-53.

Verboven C, Rabijns A, De Maeyer M, Van Baelen H, Bouillon R, and De Ranter C (2002) A structural basis for the unique binding features of the human vitamin D-binding protein. *Nat Struct Biol* **9:**131-136.

Wang Z, Lin YS, Dickmann LJ, Poulton EJ, Eaton DL, Lampe JW, Shen DD, Davis CL, Shuhart MC, and Thummel KE (2013a) Enhancement of hepatic 4-hydroxylation of 25-hydroxyvitamin D3 through CYP3A4 induction in vitro and in vivo: implications for drug-induced osteomalacia. *J Bone Miner Res* **28:**1101-1116.

Wang Z, Schuetz EG, Xu Y, and Thummel KE (2013b) Interplay between vitamin D and the drug metabolizing enzyme CYP3A4. *J Steroid Biochem Mol Biol* **136:**54-58.

Wang Z, Wong T, Hashizume T, Dickmann LZ, Scian M, Koszewski NJ, Goff JP, Horst RL, Chaudhry AS, Schuetz EG, and Thummel KE (2014) Human UGT1A4 and UGT1A3 conjugate 25-hydroxyvitamin D3: metabolite structure, kinetics, inducibility, and interindividual variability. *Endocrinology* **155:**2052-2063.

Weber EJ, Chapron A, Chapron BD, Voellinger JL, Lidberg KA, Yeung CK, Wang Z, Yamaura Y, Hailey DW, Neumann T, Shen DD, Thummel KE, Muczynski KA, Himmelfarb J, and Kelly EJ (2016) Development of a microphysiological model of human kidney proximal tubule function. *Kidney Int* **90:**627-637.

Xu Y, Hashizume T, Shuhart MC, Davis CL, Nelson WL, Sakaki T, Kalhorn TF, Watkins PB, Schuetz EG, and Thummel KE (2006) Intestinal and hepatic CYP3A4 catalyze hydroxylation of 1alpha,25-dihydroxyvitamin D(3): implications for drug-induced osteomalacia. *Mol Pharmacol* **69:**56-65.

Zheng XE, Wang Z, Liao MZ, Lin YS, Shuhart MC, Schuetz EG, and Thummel KE (2012) Human PXR-mediated induction of intestinal CYP3A4 attenuates 1alpha,25-dihydroxyvitamin D(3) function in human colon adenocarcinoma LS180 cells. *Biochem Pharmacol* **84:**391-401.

Footnotes

This work was supported in part by the National Institutes of Health [Grant R01 GM63666, U01 GM092676, P30 ES007033, TL1 TR000422, T32 GM007750, P30 CA21765]; and the American Lebanese Syrian Associated Charities.

Legends for Figures

Figure 1. Formation of 25OHD-3-*O*-sulfate by human liver cytosols and SULT2A1. Considering the structure of $25OHD_3$ shown in (A), sulfonation occurs preferentially at the 3-OH-position as seen from its formation by human liver cytosol and SULT2A1 (B). Derivatization with PTAD yields an adduct that, after ionization, gives a diagnostic ion at *m/z* 378 that includes the site of sulfonation (C).

Figure 2. Kinetics of $25OHD_3$-3-*O*-sulfate formation. Concentration-dependent formation of $25OHD_3$-3-*O*-sulfate by pooled human liver cytosol (A) and recombinant SULT2A1 (B) are shown. Individual data points from duplicate incubations at each substrate concentration are shown. The solid line represents the result of fitting a simple Michaelis-Menten equation to the substrate concentration - rate data. Mean parameter (K_m and V_{max}) estimates from three separate experiments for each enzyme system are shown in Table 1. The V_{max} values were normalized to the SULT2A1 protein content.

Figure 3. Time-dependent formation of $25OHD_3$ metabolites by human hepatocytes. Primary human hepatocytes pretreated for 24 hrs with DMSO (A) or 10 µM rifampicin in DMSO (B) were incubated with 50 nM $25OHD_3$ for an additional 0-24 hrs and the products analyzed for $25OHD_3$-3-*O*-sulfate (open square), $24R,25(OH)_2D_3$ (closed circle), $25OHD_3$-3-*O*-glucuronide (closed square) and $4,25(OH)_2D_3$ (open circle) by LC-MS/MS, as described in Methods. Each data point represents the mean ± S.D of three replicate hepatocyte incubations per donor. Two donors were used in the study. The mean rates of formation of each metabolite in hepatocytes (or rifampicin-treated) were: 0.16 (or 0.16) pmol/hr/10^6 cells ($25OHD_3$-3-*O*-sulfate), 0.11 (or 0.13) pmol/hr/10^6 cells ($24R,25(OH)_2D_3$), 0.01 (or 0.01) pmol/hr/10^6 cells ($25OHD_3$-*O*-

glucuronide) and 0.03 (0.04) pmol/hr/10^6 cells (4,25$(OH)_2D_3$; measured after β-glucuronidase treatment).

Figure 4. Association between *SULT2A1 rs296361* and SULT2A1 protein content and 25OHD$_3$ sulfonation rate in human liver. Cytosol was isolated from 258 human livers for quantitation of SULT2A1 protein content (A) and 25OHD$_3$ 3-*O*-sulfonation rate (B). Mean ± SD data for rs296361 G>A genotypes are shown. Group results were compared by ANOVA, followed by pairwise comparisons if the ANOVA result was significant; *, $p< 0.05$; **, $p < 0.01$. Of additional note, the comparison of 25OHD$_3$ 3-*O*-sulfonation rate for the homozygous rs296361 GG and AA groups reached near significance; $p = 0.052$ with post-hoc analysis.

Figure 5. Correlation between cytosolic 25OHD$_3$-3-sulfonation rate and SULT2A1 protein content and DHEA sulfonation rate in human liver. Cytosol was isolated from 258 human livers for quantitation of SULT2A1 protein content, 25OHD$_3$ 3-*O*-sulfonation rate and DHEA 3-sulfonation rate. Linear regressions between 25OHD$_3$ 3-*O*-sulfonation rate and SULT2A1 protein content (A; $r^2 = 0.22$) and between 25OHD$_3$ 3-*O*-sulfonation rate and DHEA 3-sulfonation rate (B; $r^2 = 0.27$) are shown.

Figure 6. Detection of 25OHD$_3$-3-*O*-sulfate in human plasma and bile by LC-MS/MS. Biological samples were subjected to SPE and LC-MS/MS analysis (A) or SPE, derivatization with DAPTAD and LC-MS/MS analysis (B), as described in Methods. Peaks correspond to the d_6-25OHD$_3$-3-*O*-sulfate and 25OHD$_3$-3-*O*-sulfate analytes are shown.

Figure 7. Binding of 25OHD-3-*O*-sulfate to rat vitamin D binding protein. A competitive binding assay was performed as described in Methods. A range of amounts of 25OHD$_3$, 25OHD$_3$-3-*O*-sulfate and 25OHD$_3$-3-*O*-glucuronide were incubated with ^{3}H-25OHD$_3$ and rat

DBP and the percent ^{3}H-25OHD$_3$ bound was calculated for each amount of unlabeled 25OHD$_3$-3-*O*-sulfate. EC50 values from a single binding site model were: 0.82 pmol (25OHD$_3$); 0.72 pmol (25OHD$_3$-3-*O*-sulfate); and 0.74 pmol (25OHD$_3$-3-*O*-glucuronide).

Figure 8. Metabolic pathways (oxidation and conjugation) of 25OHD$_3$ and their corresponding enzymes in human liver.

Tables

Table 1. Kinetic parameters for 25OHD$_3$-3-*O*-sulfate formation *in vitro*.

	Human Liver Cytosol	SULT2A1
V_{max} (pmol/min/mg)	24.0 ± 1.88	
V_{max} (pmol/min/nmol)	17.7 ± 1.38	21.3 ± 3.88
K_m (µM)	3.43 ± 0.02	3.36 ± 1.10
CL_{int} (µL/min/mg)	7.00 ± 0.54	
CL_{int} (µL/min/nmol)	5.15 ± 0.40	6.59 ± 1.13

Parameter values shown are mean ± S.D of three independent experiments conducted on different days. A simple Michaelis-Menten model was fitted to the data. Pooled human liver cytosol was prepared from different randomly selected livers (n = 10). Cytosolic V_{max} and Cl_{int} values normalized for total protein (mg) and specific SULT2A1 content (nmol) are presented. SULT2A1 protein was a recombinantly expressed, purified product obtained from R&D Systems.

Table 2. Multivariate regression analysis of human cytosol 25OHD$_3$ 3-sulfonation activity [1]

Characteristic	**β-coefficient in full model [2]**	**Significance in full model *(P-value)***	**Variability explained [3] *(R^2)***
Fully adjusted model		2.2×10^{-16}	0.47
rs296361 (additive effect)	0.50 ± 0.10	4.8×10^{-7}	
Gender (male ref)	-0.11 ± 0.10	0.27	
Age	-0.004 ± 0.003	0.10	
Ethnicity (white ref)	-0.28 ± 0.32	0.37	
Liver bank (UW ref)	-1.59 ± 0.14	2.0×10^{-16}	
Storage time	-0.03 ± 0.01	7.1×10^{-3}	

[1] Variability in log liver cytosolic 25(OH)D$_3$ sulfonation rate explained by predictors in a multiple linear regression. A subset (n = 226) of the overall dataset (n = 258) was included; 32 excluded because of missing age. The significance of the association of each variable with log 25(OH)D$_3$ sulfonation rate is indicated by the p-value and determined using a likelihood ratio test.

[2] Values are β-coefficients ± SE from a multiple linear regression model. β-coefficients are determined as change of log 25(OH)D$_3$ sulfonation rate (pmol/min/mg) per unit change of the predictor variable, when all other predictor variables are held constant.

[3] The goodness of fit of a multiple linear regression, on a scale of 0 to 1, as reflected in the R^2 value for the fully adjusted model of log 25(OH)D$_3$ sulfonation rate as the outcome variable and all predictors in the table: rs296361, gender, age (yrs), ethnicity, liver bank and duration of tissue storage (mo). Reference groups for categorical variables shown in parentheses.

DMD Fast Forward. Published on January 17, 2018 as DOI: 10.1124/dmd.117.078428
This article has not been copyedited and formatted. The final version may differ from this version.

Figures

Figure 1

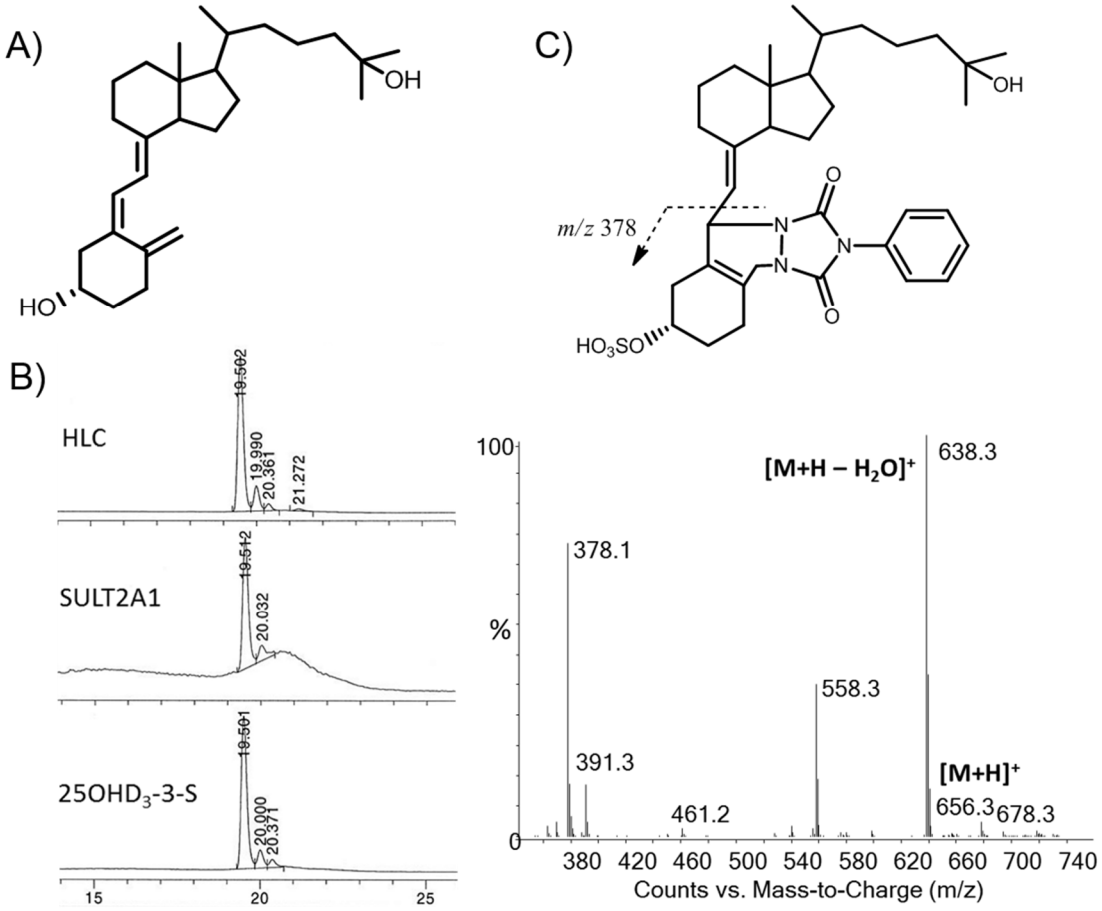

DMD Fast Forward. Published on January 17, 2018 as DOI: 10.1124/dmd.117.078428
This article has not been copyedited and formatted. The final version may differ from this version.

Figure 2

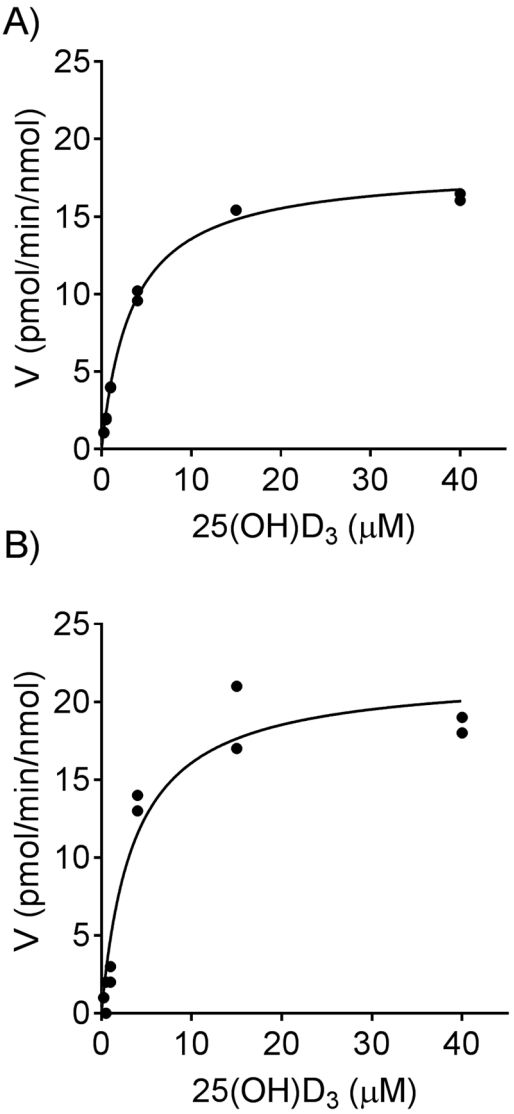

DMD Fast Forward. Published on January 17, 2018 as DOI: 10.1124/dmd.117.078428
This article has not been copyedited and formatted. The final version may differ from this version.

Figure 3

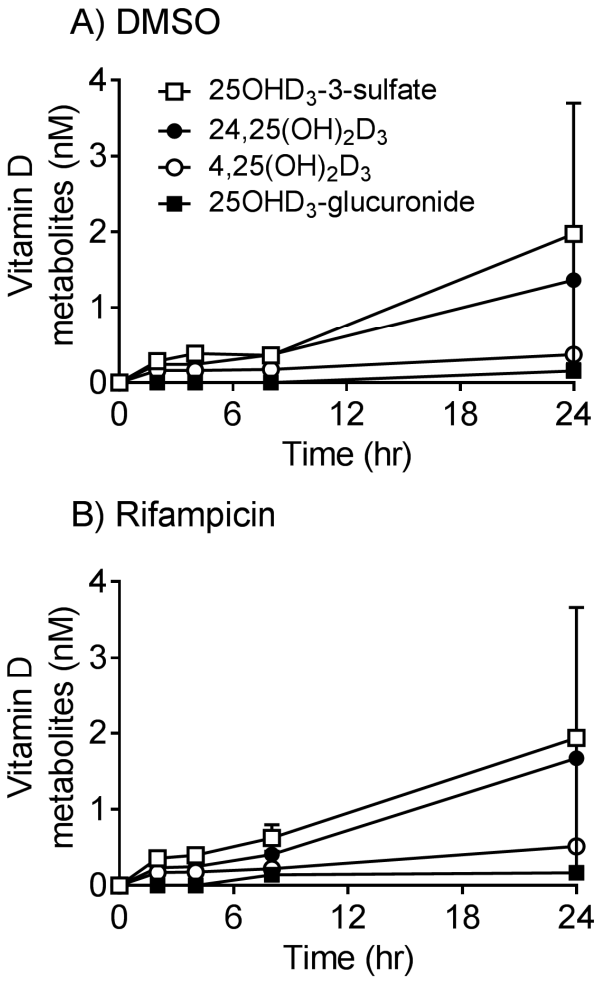

DMD Fast Forward. Published on January 17, 2018 as DOI: 10.1124/dmd.117.078428
This article has not been copyedited and formatted. The final version may differ from this version.

Figure 4

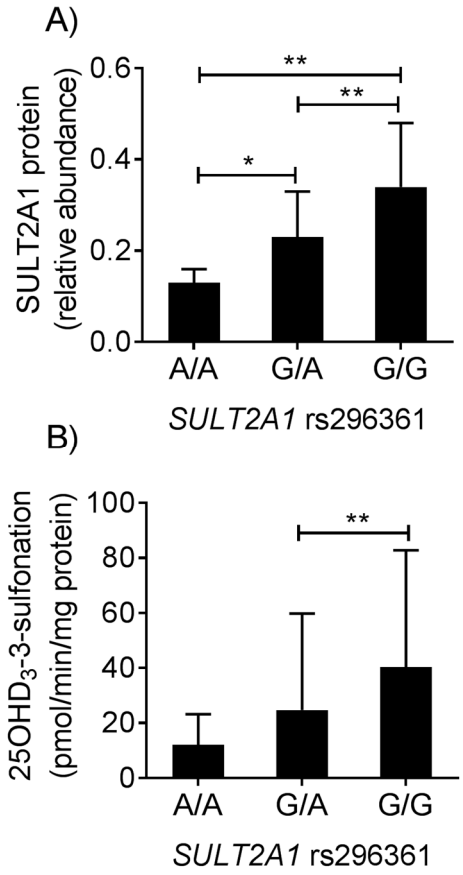

DMD Fast Forward. Published on January 17, 2018 as DOI: 10.1124/dmd.117.078428
This article has not been copyedited and formatted. The final version may differ from this version.

Figure 5

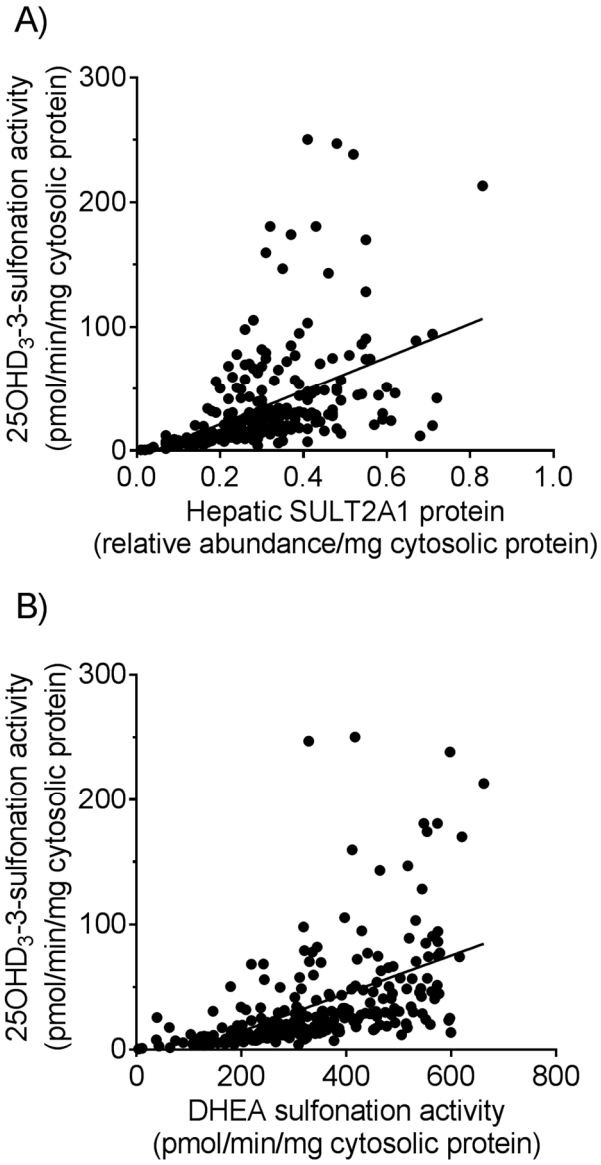

DMD Fast Forward. Published on January 17, 2018 as DOI: 10.1124/dmd.117.078428
This article has not been copyedited and formatted. The final version may differ from this version.

Figure 6

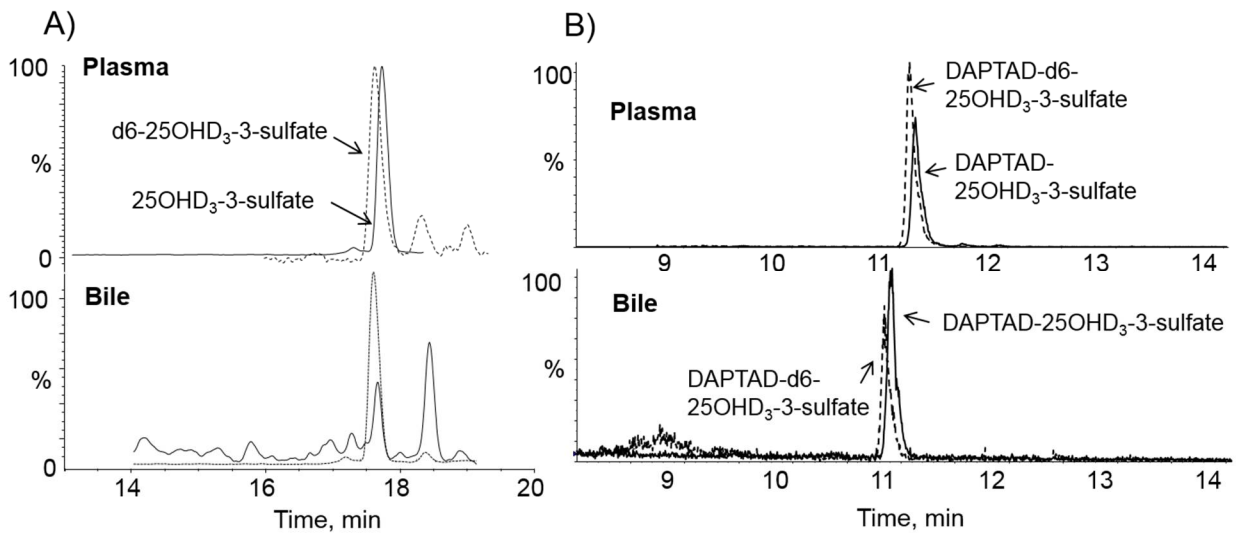

DMD Fast Forward. Published on January 17, 2018 as DOI: 10.1124/dmd.117.078428
This article has not been copyedited and formatted. The final version may differ from this version.

Figure 7

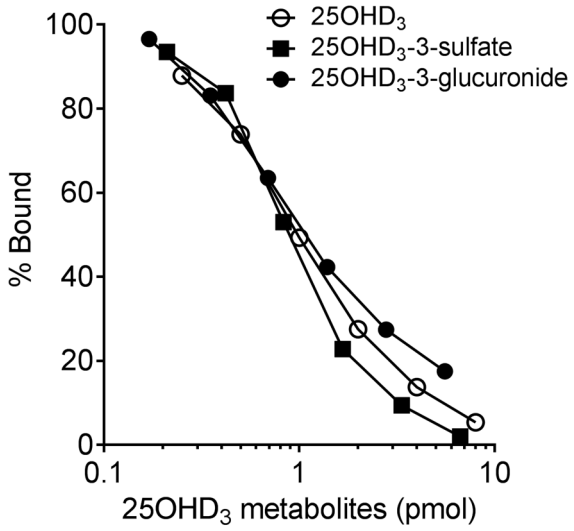

DMD Fast Forward. Published on January 17, 2018 as DOI: 10.1124/dmd.117.078428
This article has not been copyedited and formatted. The final version may differ from this version.

Figure 8